

Continuous-Flow Tubular Crystallization in Slugs Spontaneously Induced by Hydrodynamics

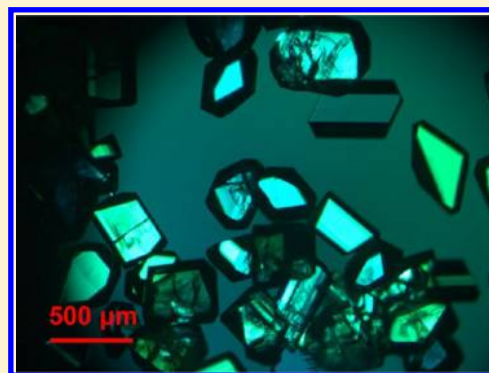
Mo Jiang,[†] Zhilong Zhu,[†] Ernesto Jimenez,[†] Charles D. Papageorgiou,[‡] Josh Waetzig,[‡] Andrew Hardy,[‡] Marianne Langston,[‡] and Richard D. Braatz^{*,†,‡}

[†]Massachusetts Institute of Technology, 77 Massachusetts Avenue, Cambridge, Massachusetts, 02139, United States

[‡]Millennium: The Takeda Oncology Company, Process Chemistry Research & Development, 35 Landsdowne Street, Cambridge, Massachusetts 02139, United States

S Supporting Information

ABSTRACT: A novel continuous crystallizer design is described with the potential to provide improved control of crystal properties, improved process reproducibility, and reduced scale-up risk. Liquid and gas are introduced into one end of the tube at flow rates selected to spontaneously generate alternating slugs of liquid and gas that remain stable while cooling crystallization occurs in each liquid slug. Mixing within each stable self-circulating slug is maximized by controlling the slug aspect ratio through specification of liquid and gas flow rates. The crystallizer is designed so that nucleation and growth processes are decoupled to enhance the individual control of each phenomenon. Coaxial or radial mixers combine liquid streams to generate seed crystals immediately upstream of the growth zone where nucleation is minimized, and crystal growth is controlled by the varying temperature profile along the length of the tube. The slug-flow crystallizer design is experimentally demonstrated to generate large uniform crystals of L-asparagine monohydrate in less than 5 min.



1. INTRODUCTION

Compared to batch and semibatch crystallizers, continuous-flow crystallizers have the potential for higher reproducibility, process efficiency, and flexibility, as well as lower capital and production cost.^{1–8} Many continuous-flow crystallizer designs have been proposed in recent years with the goals of improving pharmaceutical processing or control of crystal product properties. For example, a continuous oscillatory baffled crystallizer has been proposed that employs a piston to agitate the crystal slurry in a long pipe with baffles.² Such a crystallizer can typically operate at lower shear rates than a single stirred-tank crystallizer but is limited to lower solids densities and effective viscosities and has limited degrees of freedom for feedback control. An alternative design that employed laminar flow through a tube was demonstrated for paracetamol crystallization, but it was warned that inducing crystallization in a continuous slurry undergoing laminar flow in a tube by cooling through its walls was very prone to clogging for some solute–solvent systems.⁶ With the notion that the best control of crystal size distribution should be obtained in a continuous-flow design that has negligible back-mixing with a residence time distribution approaching that of an ideal plug-flow crystallizer, several designs have tried to generate plug flow-like conditions. One continuous crystallizer design consists of slurry flowing through a tube with Kenics-type static mixers through its length to induce a more uniform velocity profile, with improved controllability obtained by introducing antisolvent at multiple points along the tube length.¹ A tubular crystallizer less prone to clogging ensured plug-flow behavior by forcibly segmenting the

flow into liquid slugs separated by an immiscible fluid.^{3–5,9} Because of recirculation, the slurry in each slug is mixed even in the absence of any static mixer.^{10,11} However, the separation of immiscible solvent takes additional process time when multiple liquids are used, and the slug production devices, usually with more than three channels, were relatively complicated. A significant advantage of all of these continuous-flow crystallizer designs is the lack of a stirring blade, resulting in negligible attrition compared to the mixed-suspension mixed-product-removal crystallizers widely employed for inorganic crystallization.¹²

Most existing continuous-flow crystallizers are not specifically designed to provide many degrees of freedom for the control of crystal shape and size distribution in the presence of process disturbances and variations in crystallization kinetics associated with changes in contaminant profile of the feed streams. An improved continuous-flow crystallizer design would minimize operational problems while retaining the advantages of the best previous continuous crystallizers. At same time, there are advantages to continuous-flow designs that enable the direct application of best-practices operations developed for the optimal control of batch and semibatch crystallization.

Toward these goals, this paper describes the design and implementation of a slug-flow crystallizer in which a multiphase mixture of liquid and gas in a tube spontaneously separates into

Received: November 17, 2013

Revised: January 2, 2014

Published: January 7, 2014

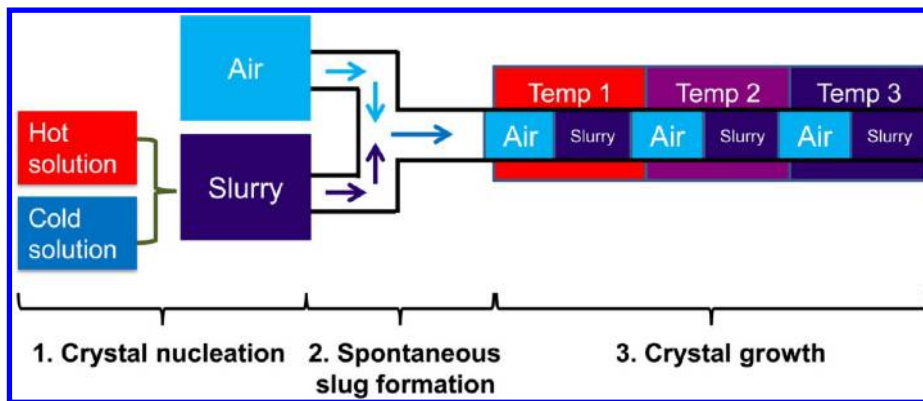


Figure 1. Schematic of slug-flow cooling crystallization. Crystal nucleation is induced by combining hot and cold LAM-aqueous solutions (photographs in Figure 2). Slug formation spontaneously occurred by combining LAM slurry and air streams (Figure 3a). Crystal growth occurs in the slurry in each slug going through the tube for a specified residence time (Figure 3b).

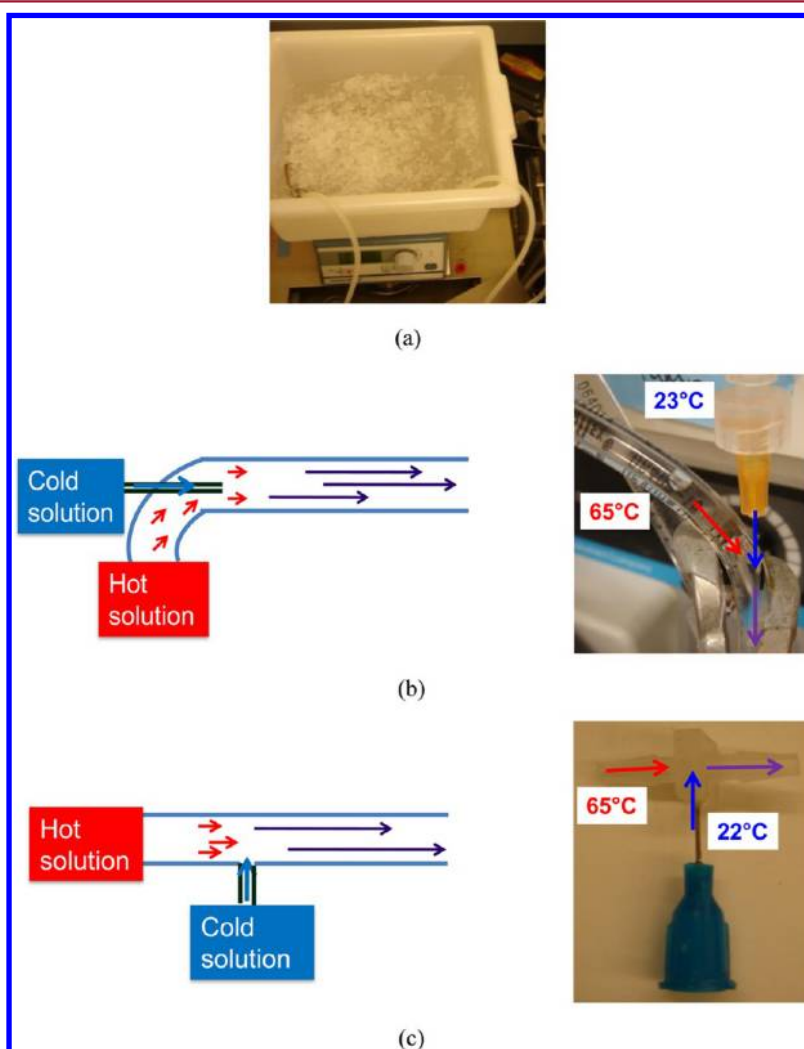


Figure 2. Photographs and schematics of setup for nucleation induced by cooling: (a) laminar flow tube; (b) coaxial mixer, the inner diameters of the two inlets are 3.1 mm (hot) and 0.26 mm (cold), respectively; (c) radial mixer, the inner diameters of the two inlets are 2 mm (hot) and 0.3 mm (cold), respectively.

slugs of liquid or slurry separated by slugs of gas.^{13–19} The slug-flow crystallizer has all the advantages of a segmented-flow crystallizer but does not require any specialized equipment to induce slug formation and avoids the use of liquid/liquid separators. In the proposed design, *hydrodynamically stable slugs*

form spontaneously immediately upon the contact of the liquid/slurry and the gas. This paper demonstrates the crystallizer design for a cooling crystallization, which is inherently more challenging than antisolvent crystallization due to the latter’s easier nucleation to generate seed crystals.

2. EXPERIMENTAL METHODS AND EQUIPMENT SETUP

For better control of product crystal size distribution (CSD), the cooling crystallization process is decoupled into three parts: crystal nucleation, slug formation, and crystal growth (Figure 1). Nuclei were generated within laminar flow by direct cooling, or within a coaxial or radial jet mixer by mixing hot and cold solutions. The slurry stream containing nuclei acting as seed crystals are combined with an air stream at flow rates selected to spontaneously form stable slugs. The motion of the slug through the tube mixes the solution without requiring any of the stirring blades that cause attrition in mixed-tank crystallizers. With each slug going through the tube with the same residence time, and with no stirring blades to cause attrition, the crystals in the slugs would be expected to grow to a large uniform size. The following experimental methods and equipment setup were selected to demonstrate the feasibility of this process design.

The solute is *L*-asparagine monohydrate (LAM, purity $\geq 99\%$ (TLC), from Sigma Aldrich), and the solvent is deionized (DI) water, which were selected because this solute–solvent combination is a well-studied model system that is challenging due to the very strong tendency of LAM crystals (product form, Figure A1, Supporting Information) to aggregate in this solvent.²⁰

2.1. Nuclei Generation. In a preliminary experiment, a high solids amount (high initial concentration, 0.16 g of LAM/g of DI, as shown in Table 1) in each slug was used to demonstrate slug stability and

Table 1. Main Experimental Conditions for Cooling Nucleation^a

experiment	preliminary	coaxial	radial
concentration of hot stream (g of LAM/g of DI)	0.16 or 0.09	0.16	0.16
concentration of cold stream (g of LAM/g of DI)	N/A	0.02	0.02
temperature of hot stream (°C)	65 or 44	65	66
temperature of cold stream (°C)	N/A	23	22
pump for hot stream	peristaltic	peristaltic	peristaltic
pump for cold stream	N/A	peristaltic	syringe
tubing for hot and cold streams	Tygon	Tygon	BioPharm
volumetric flow rate of hot stream (mL/min)	23.5	7.2	3.7
volumetric flow rate of cold stream (mL/min)	N/A	6.8	3.3
average velocity of hot stream (m/s)	0.05	0.02	0.02
average velocity of cold stream (m/s)	N/A	2.14	0.78
nucleation site (mixer)	Figure 2a	Figure 2b	Figure 2c
mixer inner diameter of hot inlet (mm)	3.1	3.1	2
mixer inner diameter of cold inlet (mm)	N/A	0.26	0.3

^aThe preliminary experiment did not have a cold stream (the hot stream was directly cooled in an ice bath; see Figure 2a). “Peristaltic” refers to a peristaltic pump (Masterflex pump drive 7521-40, Easy Load II pump head with model # 77200-50), and “Syringe” refers to a syringe pump (model NE-4000, from New Era Pump Systems, Inc.). “Tygon” refers to Masterflex Tygon tubing, and “BioPharm” refers to Masterflex BioPharm Plus platinum-cured silicone tubing. The volumetric flow rate reported for the syringe pump was precalibrated, and the volumetric flow rate reported for the peristaltic pump was estimated from the mass flow rate and temperature measured right before or after the experiment. The average velocities are calculated from the volumetric flow rates and mixer inner diameters.

CSD improvement in the growth stage. In another preliminary experiment, a low solids amount (low initial concentration, 0.09 g of LAM/g of DI, as shown in Table 1) was applied to facilitate in-line and off-line imaging and to compare the nucleation obtained from coaxial and radial mixers, to identify the most promising mixer type for subsequent experiments.

The nucleation experimental conditions are listed in Table 1. For the radial mixing experiment (LAM nuclei were generated by combining hot and cold saturation solutions (66 °C, 0.16 g of LAM/g of DI; and 22 °C, 0.02 g of LAM/g of DI, respectively) through a coaxial or radial jet mixer (Figure 2b,c). This approach, first demonstrated in ref 20, contrasts with other continuous tubular cooling crystallizations that require a separate batch crystallizer to produce seed crystals to feed into the continuous crystallizer. Peristaltic pumps enable simple operation of tubing at high temperature, while a syringe pump provides smooth flow rates. A peristaltic pump (Masterflex pump drive 7521-40, Easy Load II pump head with model #77200-50) and a silicone tube (Masterflex BioPharm Plus platinum-cured silicone tubing, 3.1 mm inner diameter) were used to transfer hot solution to the mixer at a rate of about 3.7 mL/min. The tubing choice was based on the following criteria: low extractable and spallation, high temperature endurance, surface hydrophobicity (a more convex water slug shape is obtained by using a more hydrophobic surface),²¹ and long life of the pump tubing. Around the pump head, a silicone tube with smaller inner diameter (2 mm) was used to increase the pump rotation rate for the same flow rate, to reduce the amplitude of flow pulsations. A syringe pump (model NE-4000, from New Era Pump Systems, Inc.) was used to transfer cold solution to the mixer at a rate of 3.3 mL/min. The operational details of the other experiments in Table 1 are similar to the radial mixing experiment but with the different values given in the associated column of the table.

2.2. Slug Generation. A key element in the proposed crystallizer design is to exploit the hydrodynamically stable spontaneous generation of slugs. Many hydrodynamically stable flow regimes can occur when a liquid and gas are combined in a tube, as shown in Figure 3,^{15,16,22} with the stability of the flow regimes determined by

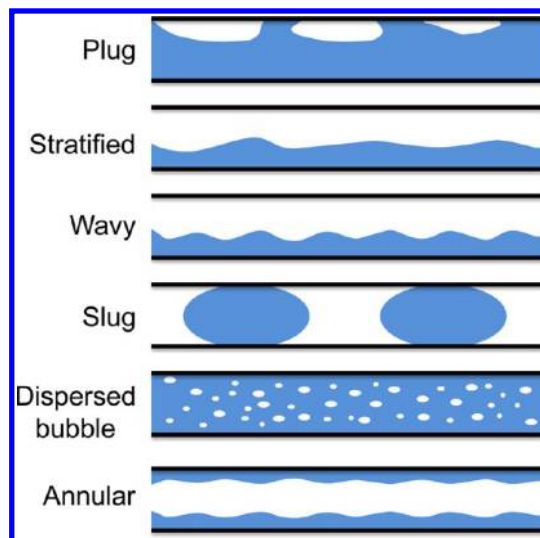


Figure 3. Schematics of hydrodynamically stable flow patterns of a gas (white color) and liquid (blue color) mixture in a horizontal round tubing. The notations and images of the flow were based on ref 22. The air and liquid in slug flow can swap places depending on the affinity of the liquid for the material on the inner surface of the tube; for example, a water slug with a strongly hydrophobic surface would appear as shown, with convex/roundish water slugs moving through the tube. For a strongly hydrophilic surface with water as the liquid, the air slugs would be convex. Regardless of surface affinities, the slugs become asymmetric at sufficiently high velocities, as observed in Figure 10.

the ranges of inlet gas and liquid flow rates, tubing diameter, and fluids properties. For crystallization from liquid solution, most of the flow regimes have relatively poor spatial mixing of the liquid and allow liquid solution to remain close to the tube walls for long periods of time, which would encourage crystallization on the surface of the inner

tube (aka fouling), eventually clogging the tube. In contrast, slug flow has an internal circulation of liquid¹¹ (see video in Supporting Information) that limits the time that liquid stays close to the tube wall, which results in the fluid dynamics within each slug operating like a small well-mixed crystallizer, with limited fouling.

Figure 4a shows an experimental demonstration of the spontaneous formation of hydrodynamically stable slugs after streams of slurry and

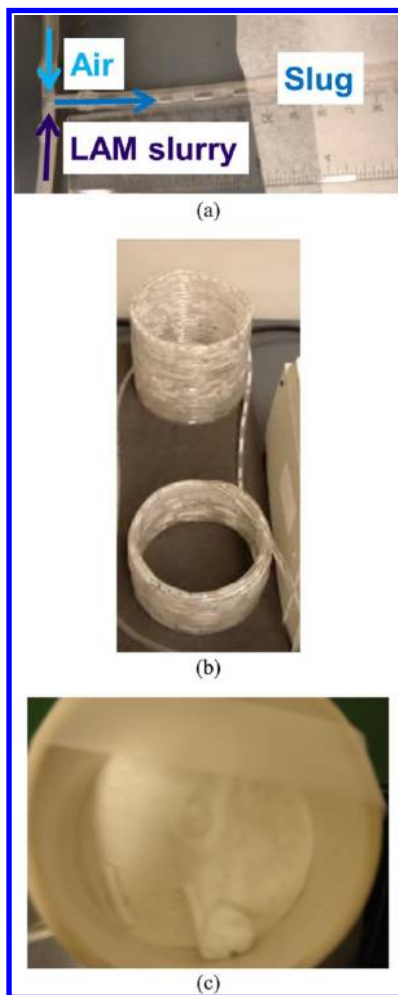


Figure 4. (a) Slug formation from streams of LAM slurry and air through a T mixer. The white slugs contain LAM-aqueous slurry, and the transparent slugs are air. (b) Slurry-containing slugs in the growth stage. The white slugs have high solids densities in this photograph. (c) Crystals in the funnel after filtration obtained under operations of high solids density in each slug.

air are passed through two branches of a T mixer that had a similar inner diameter as the tubes. Stable slugs were maintained throughout crystallization within each slug as it transports through the tubing to its exit. Air was transferred to the mixer through the same peristaltic pump with dual pump heads, with flow oscillation suppressed by offsetting their rollers, and a silicone tube with filters (pore sizes 3 and $0.2\ \mu\text{m}$) to prevent dust particles from getting into the tubes at the pump heads, and from contacting slurry at the mixer, respectively. Within a large hydrodynamically stable regime¹⁶ for slugs in a 3.1 mm (inner diameter) tube, the length ratio of liquid and gas slugs was adjustable by specifying the flow rates (or pump rotation rates) between slurry and air. A pump rpm ratio of 1:1 between hot solution and air was used to generate stable liquid slugs of similar sizes with all aspect ratios of about 1 (Figure 5a,b). A horizontal wrapping of tubing around a bucket produced hydrodynamically stable slugs with no combination or partitioning (Figures 4b and 5a,c).

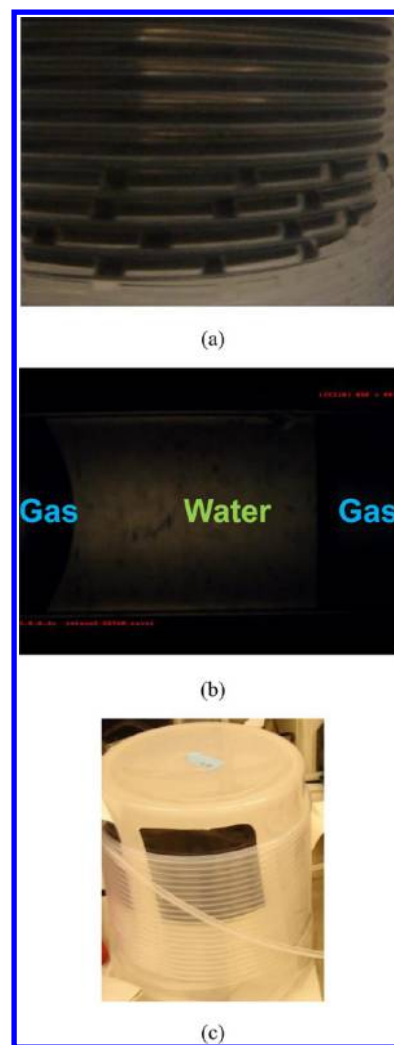


Figure 5. (a) Photograph of stable water slugs (aspect ratio about 1) separated by air slugs (aspect ratio about 4) in packed silicone tube, with black background to improve contrast. (b) Microscope image of water slug (slug in the center) and parts of air slugs (dark regions at both edges) inside a silicone tube. The flow direction is from left to right. The front of the water slug is less curved toward the flow direction than the back,¹⁴ as indicated from the thickness of black shades at water/air interfaces. At higher flow rates, the shape of the water slug would be dominated by the velocity (e.g., the drag from wall) rather than the hydrophobicity of the tubing material. (c) Horizontal wrapping of silicone tube around a cylinder of the same diameter. The photograph (a) is a close-up of (c) indicated by the edge of the black background.

2.3. Crystal Growth. The growth experimental conditions were reported in Table 2. Again the radial mixing experiment was used to justify the optimized design. The residence time after slug formation was on the order of 5 min (to prevent generation of a large amount of waste materials) in 15.2 m of transparent hydrophobic silicone tube (Dow Corning Pharma-80 tubing, 3.1 mm inner diameter). While the slugs were moving inside the silicone tube toward the exit, videos of them were recorded under an in-line trinocular stereomicroscope (microscope model #XV331AC20C, from Cyber Scientific Corp.; camera model #DFK 22BUC03, from The Imaging Source, LLC) at 1 m before the exit. After the slurry slugs exited the end of tube, they were collected one by one into polystyrene wells (1.5 cm diameter, with the aqueous slugs covered with corn oil after collection to suppress evaporation) for off-line imaging under the stereomicroscope.

Crystallizations are generally more poorly mixed for higher solids densities. Since each slug operates as a small well-mixed batch

Table 2. Experimental Conditions for Slug Formation and Growth by Cooling^a

experiment	preliminary	coaxial	radial
pump for air stream	peristaltic	peristaltic	peristaltic
pump rotation rate for air stream (rpm)	66	78	53.4 (dual head)
tubing for slug movement	Tygon	Tygon	Pharma-80
tubing length (m)	15.2	15.2	15.2
residence time (min)	1.7	2.9	5.0
tube inner diameter (mm)	3.1	3.1	3.1

^a“Peristaltic” and “Tygon” are the same terms as in Table 1, and “Pharma-80” refers to Dow Corning Pharma-80 tubing. Residence time counts the time between when the hot solution reaches the mixer and the exit of the tubing.

crystallizer, each slug will not be as well mixed for a high solids density, in which case a fines dissolution step can be inserted into the crystal growth stage to enlarge the final product crystals and reduce aggregation. The end stage of the preliminary experiment had fines dissolution implemented as a fast heating of the slurry slugs to 50 °C, followed by going through 2 m of tubing in each of the two temperature baths at 39 and 22 °C, respectively, and then to room temperature (Figure 6).

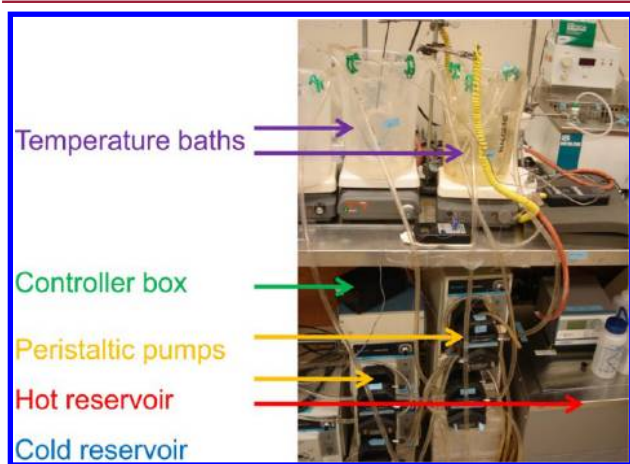


Figure 6. Photograph of the experimental setup with two temperature baths. The hot reservoir is in a temperature-controlled bath (lower right), and the cold reservoir is in an ice bucket at the lower left (not shown in the picture). Each of the two temperature baths at the top of the photograph is controlled with only one dual-head peristaltic pump using Proportional-Integral controllers tuned by Internal Model Control.^{30,31} The dual head transfers both inlet and outlet water, keeping the water level of the reservoir constant. The temperature of the slugs in the tube increases or decreases relatively slowly due to the low thermal conductivity of the tube wall. Only one temperature bath is needed for coarse temperature control; additional temperature baths enable finer tuning of the spatial temperature profile of the slugs as they move through the tube.

The temperature in each bath was held constant using peristaltic pumps (same model as before) and hot and cold water reservoirs (Figure 6), controlled with Proportional-Integral controller tuned as in past studies.²³ The temperature baths were not used in experiments with coaxial and radial mixing, as the product crystals from those experiments were uniformly large without fines dissolution.

3. RESULTS AND DISCUSSION

Below are results and discussion from the experimental demonstrations of the slug-flow crystallizer that include (1) a nonmonotonic spatial temperature profile to reduce aggregation and promote growth, (2) a comparison of coaxial and

radial mixers for in situ generation of seed crystals, and (3) the improvement of hydrodynamics for reducing variations in product quality.

3.1. Preliminary Experiment with Temperature Baths to Reduce Aggregation and Promote Growth. After crystal nucleation in a tube under laminar flow (no mixer, Re number of about 150; see Figure 2a) and slug formation (Figure 4a), the solids amount increases in the slugs as they move along the tube length, indicated by the whiter color of slurry slugs (Figure 4b, top) observed visually after a short period of growth. Under high initial solute concentrations, the slugs were able to carry 12.3 wt % crystals in the slurry, with crystals nearly occupying the whole slug (Figure 4b) at a reasonably fast flow rate (Table 1). The total yield (mass of product crystals/total mass of solute) from this preliminary experiment was 87%, close to the theoretical yield of a batch cooling experiment from the same hot solution (87.5%).

The final product crystals after growth from laminar flow nucleation were small and aggregated (Figure 7a) (LAM has a strong tendency toward aggregation²⁰). Heating followed by

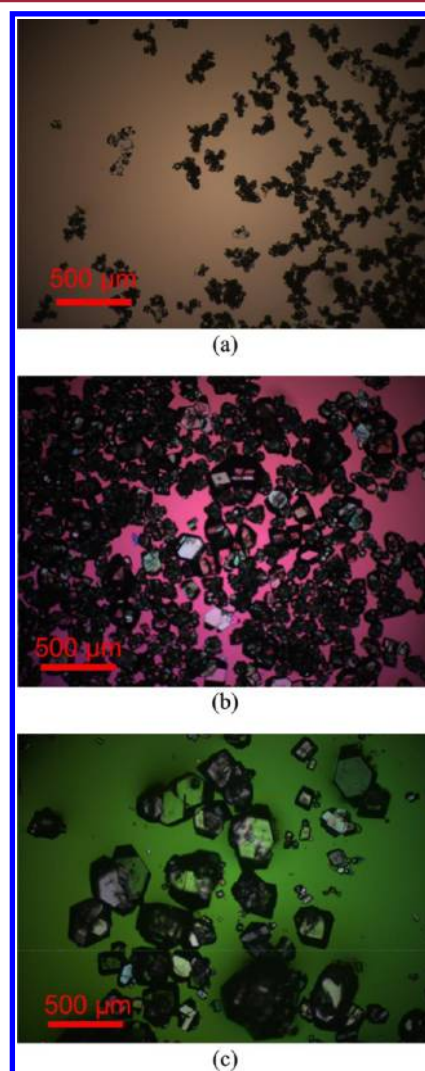


Figure 7. Microscope (with polarizers) images of product crystals from the preliminary experiment (after laminar flow nucleation and growth in slugs) with (a) no heating; (b) heating to 50 °C followed by natural cooling in the tubing; (c) heating to 50 °C followed by two temperature baths of set temperatures (39 and 22 °C).

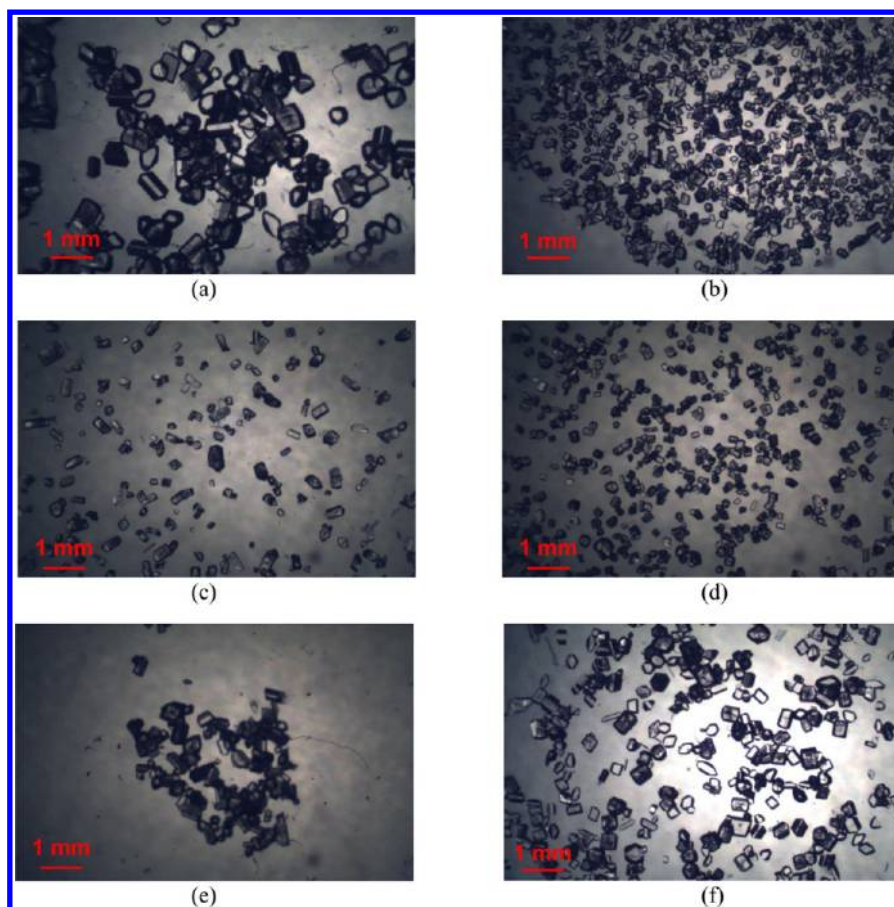


Figure 8. Stereomicroscope images of product crystals with nucleation induced by coaxial mixing in slug number (a) 21, (b) 81, (c) 141, (d) 201, (e) 261, (f) 311 (last slug). The scale bar = 1 mm. Detailed experimental conditions are provided in the coaxial experiment column in Tables 1 and 2.

natural cooling in the tubing after the first stage of growth was expected to increase the crystal size,^{24,25} which was observed experimentally (Figure 7b). Heating followed by cooling in two baths of controlled temperatures was able to further increase the average crystal size and reduce aggregation (Figure 7c). Some small crystals remained, which motivated the implementation of mixers to provide better control of nucleation, which is described next.

3.2. Improved Hydrodynamics (e.g., Coaxial Mixing) to Improve Nucleation from Laminar Flow. The product crystals obtained when nucleation was induced by coaxial mixing (Figure 8) improved the seed crystal quality (Figure 9), with less aggregation and narrower CSD in each slug, compared to nucleation in laminar flow (Figures 7a and A2, Supporting Information). Crystals nucleated by impinging a hot and a cold solution at an approximately equimolar ratio (Table 1) in a small volume can be more uniform in size than crystals nucleated by cooling from a single solution, as high local supersaturation (much higher than the average supersaturation) can be obtained near the interface between hot and cold solutions when the thermal diffusivity is much larger than the molecular diffusivity, as experimentally demonstrated and explained in a previous study.²⁰ By combining two streams, the coaxial mixer also has more intense mixing than would be obtained using one stream,²⁶ with a $Re \approx 600$, which is expected to lead to more uniform-sized crystals due to more crystals following a similar supersaturation trajectory in the crystal phase diagram.

While each slug obtained using the coaxial mixer (Figure 8) had orders-of-magnitude less aggregation than the preliminary

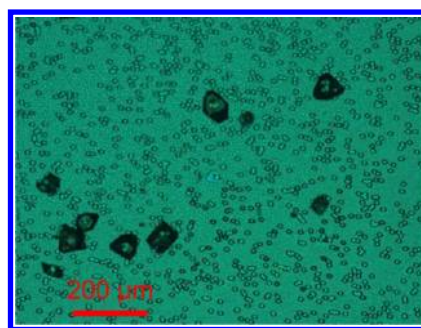


Figure 9. Seed crystals generated by cooling nucleation in a coaxial mixer. The background is a membrane filter with a pore size of 10 μm . The flow setups are in Figure 2b. Although the quantitative size of measured seed crystals is a combination of both nucleation and growth (with local supersaturation not easy to measure at fine spatial resolution), this image does qualitatively show the coaxial mixing reduces crystal aggregation and CSD width compared to laminar flow.

experiment (Figure 7), the crystal number per unit volume and mean crystal size were variable from one slug to another (Figure 8). With nucleation using a coaxial mixer, the crystal size distribution was narrow within nearly each slug (Figure 8a–f). The variation in size of crystals before slug formation (Figure 9) is similar to that within a single slug (Figure 8, Table 3), which suggests that the mixing within each slug (from internal recirculation¹⁹) may be sufficient for maintaining a spatially uniform environment of temperature and concentration after nucleation. In particular, if the mixing had not been

Table 3. Product Crystal Size and Shape Statistics for Slug-Flow Crystallization, for Nucleation Using Coaxial Mixing Corresponding to the Experimental Results Reported in Figure 8^a

slug number	21	81	141	201	261	311	All
crystal image	Figure 8a	Figure 8b	Figure 8c	Figure 8d	Figure 8e	Figure 8f	Figure 8a–f
crystal mean length (μm)	442	205	231	279	341	318	303
standard deviation, length (μm)	100	62	107	81	132	96	99
crystal mean width (μm)	316	136	144	184	217	222	203
standard deviation, width (μm)	82	46	58	52	69	76	65
correlation coefficient of length and width	0.43	0.21	0.72	0.58	0.65	0.54	0.52
coefficient of variation in length	0.23	0.30	0.46	0.29	0.39	0.30	0.34
coefficient of variation in width	0.26	0.34	0.40	0.28	0.32	0.34	0.33

^aThe correlation coefficient of length and width varies widely from slug to slug, which indicates a wide range of crystal aspect ratios among different slugs (a correlation coefficient of length and width of 1 would correspond to all crystals having exactly the same aspect ratio).

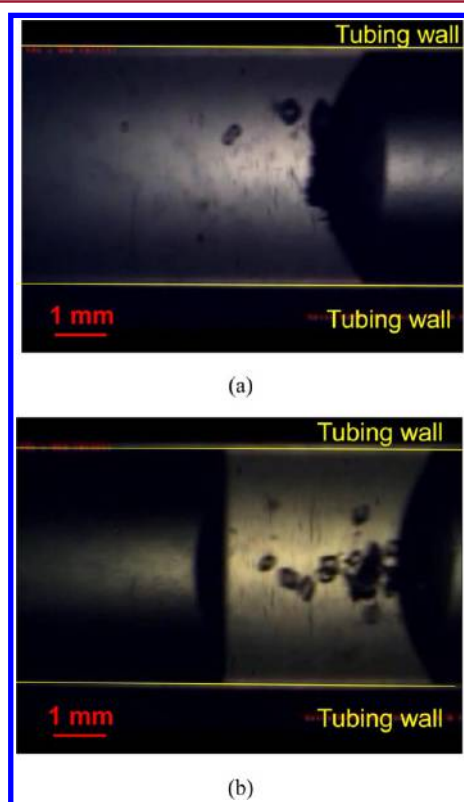


Figure 10. In-line stereomicroscope images of crystals in slugs with an aspect ratio of about (a) 4 (the slug is too long to fit into the image and is off to the left) and (b) almost 1. The scale bar \approx 1 mm. Relatively low solids density was used in both experiments so that the crystals could be clearly imaged.

sufficient, there would have been a small number of crystals much larger than shown in Figure 8, such as observed at the bottom of poorly mixed batch crystallizers. The slug-to-slug variability suggested that some experimental component was inducing oscillations to the experimental system, which led to an effort to reduce flow pulsations from the peristaltic pumps (the experimental details are in sections 2.1 and 2.2, with the results discussed in next section).

3.3. Improved Hydrodynamics (e.g., Reducing Flow Variation) to Reduce Slug-to-Slug Variability. With the objective of reducing slug-to-slug variability, flow pulsations were reduced by replacing the peristaltic pump for cold liquid solution with a syringe pump, and by implementing off-setting dual heads of the peristaltic pump for the gas flow. Since another goal was to reduce variability generally, the

slug shape was modified to improve mixing within each slug. In particular, better mixing is expected from a slug whose aspect ratio is close to 1, such as for the slugs in Figures 5b and 10b, rather than larger aspect ratios as for the slugs in Figures 4b and 10a. An aspect ratio closer to 1 was expected to make the crystals more spread out within each slug, which was experimentally confirmed (Figure 10a,b). The effect of aspect ratio on mixing within each slug was more obvious with higher flow rates.

In addition, the coaxial mixer was replaced by a radial mixer, which provides much better mixing for systems of comparable velocities.²⁷ Compared with the coaxial mixer (Figure 8a–f, Table 3), the radial mixer experiment produced similar mean aspect ratios and coefficient of variations in length and width (Figure 11a–f, Table 4) within each slug but larger mean crystal dimensions and much lower variability in crystal shape (i.e., aspect ratio) within each slug. The reduction of variability of the product crystal shape in the radial mixer experiment may be attributed to its reduced flow variability. The use of either coaxial or radial mixers reduced aggregation by orders-of-magnitude compared to laminar flow (compare Figures 8 and 11 with Figure 7).

4. CONCLUSIONS

High-quality nonaggregating LAM crystals were produced in a continuous-flow cooling crystallizer that employed alternating slugs of slurry and air moving through a tube with a residence time of 2–5 min. The most novel aspects of the experimental system are that (1) the crystals were nucleated by mixing hot and cold solutions in coaxial and radial mixers instead of rapid cooling of a single solution^{4,6} or feeding seeds obtained by batch crystallization as done in many past continuous-flow cooling crystallization studies,²⁸ and (2) the slugs were spontaneously induced by hydrodynamic forces rather than by alternating the feed between the two inlet flows.⁵ As used in some past studies,^{3,5} air was employed as the separating fluid so that no liquid–liquid separations are needed downstream from the crystallization.

The slugs generated spontaneously by hydrodynamic forces were highly uniform in size and shape, and the slugs maintained that uniformity during crystallization as the slugs moved through the tubular crystallizer. The slug size and shape were controllable by just changing the ratio of volumetric flow rates of the inlet streams of slurry and air. An in-line imaging system was employed to study the effect of slug aspect ratio, which confirmed the expectation that aspect ratios near 1 produced better mixing than larger aspect ratios. The size uniformity of the product crystals was enhanced by the introduction of

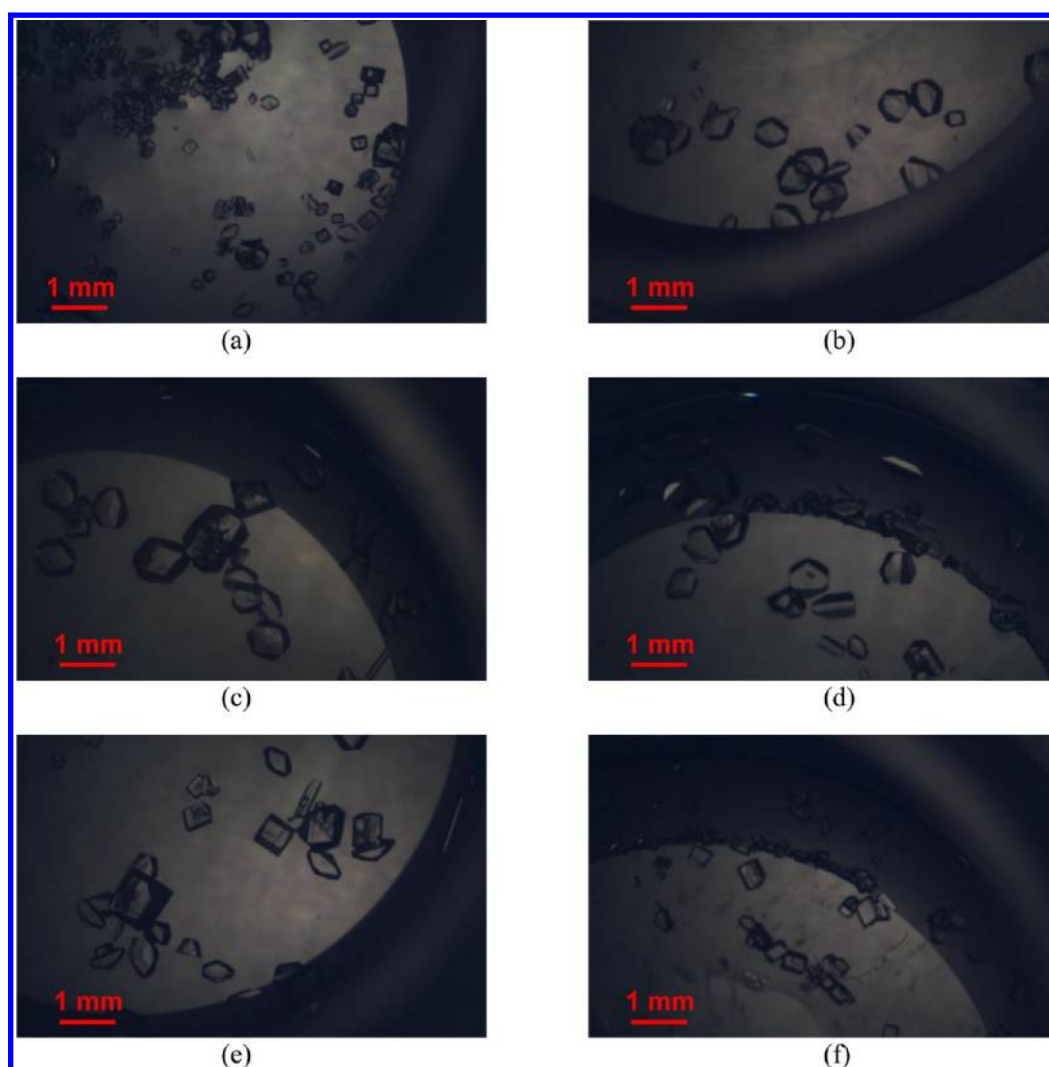


Figure 11. Stereomicroscope images of product crystals with nucleation by radial mixing in slug number (a) 16–18, (b) 106–108, (c) 286–288, (d) 466–468, (e) 646–648, (f) 726–728 (last slug). The scale bar = 1 mm. The total number of slugs is much larger than for the coaxial mixing experiments, for a similar amount of feed solutions, due to the smaller aspect ratios of the slugs. The dark ring-shape shades are due to the different refractive index between corn oil and water. Brighter areas are covered with corn oil. Crystals on top of the slurry (usually tiny) will tend to align at the interface between the oil and water. Detailed experimental conditions are provided in the radial experiment column in Tables 1 and 2.

Table 4. Product Crystal Size and Shape Statistics for Slug-Flow Crystallization, for Nucleation Using Radial Mixing Corresponding to the Experimental Results Reported in Figure 11^a

slug number	16–18	106–108	286–288	466–468	646–648	726–728	all
crystal image	Figure 11a	Figure 11b	Figure 11c	Figure 11d	Figure 11e	Figure 11f	Figure 11a–f
crystal mean length (μm)	225	479	588	545	502	325	444
standard deviation, length (μm)	103	146	202	160	181	92	152
crystal mean width (μm)	176	388	471	371	330	220	326
standard deviation, width (μm)	90	152	181	146	173	71	142
correlation coefficient of length and width	0.92	0.86	0.90	0.81	0.74	0.76	0.83
coefficient of variation in length	0.46	0.30	0.34	0.29	0.36	0.28	0.34
coefficient of variation in width	0.51	0.39	0.39	0.39	0.52	0.32	0.43

^aThe correlation coefficient of length and width is near 1 for each slug, which indicates a high consistency in aspect ratio among different slugs (a correlation coefficient of length and width of 1 would correspond to all crystals having exactly the same shape).

the coaxial or radial jet mixers to improve nucleation and by employing in-line fines dissolution involving a nonmonotonic spatial temperature profile (cooling, then heating, then cooling). The crystals grown from nuclei produced in a radial mixer were more uniform in size compared to a coaxial mixer (compare Figures 11 and 8). The high degree of mixing and small size

of each slug promoted high spatial uniformity of temperature within each slug.

The experimental system can be used to simplify scale-up as the slug volume can be selected as the same volume as the batch crystallizer used in bench-scale experiments for initial process development. The residence time of 2–5 min is orders

of magnitude shorter than the hours taken in a stirred-tank crystallization, enabled by the much higher supersaturations that can be generated within a slug while maintaining pure-growth conditions (the slug does not have a stirring blade, which is the primary source of secondary nuclei and attrition particles in a mixed-tank crystallizer). With further optimization, it is likely that the residence time could be brought down to less than 1 min. The slug-flow crystallizer has higher equipment utilization, as the experimental system can generate crystals with narrow CSD with orders-of-magnitude higher supersaturation and growth rate than obtainable using a stirred tank of the same volume. Instead of scale-up, throughput can be further increased by scale-out, that is, using more slugs. While scale-out has already been discussed many times in the literature for microscale systems,²⁹ this approach is much more industrially relevant for the length scales considered in this article, at least for the typical production rate for a pharmaceutical compound.

■ ASSOCIATED CONTENT

📄 Supporting Information

XRPD pattern and microscope images for L-asparagine monohydrate product and seed crystals, and a video showing internal circulation within water slugs with ink used as the tracer. This material is available free of charge via the Internet at <http://pubs.acs.org>.

■ AUTHOR INFORMATION

Corresponding Author

*Fax: +1-617-258-0546. E-mail: braatz@mit.edu.

Notes

The authors declare no competing financial interest.

■ ACKNOWLEDGMENTS

The authors thank Millennium: The Takeda Oncology Company for financial support. Jun Xu is acknowledged for advice on the setup of the video imaging system.

■ REFERENCES

- (1) Alvarez, A. J.; Myerson, A. S. Continuous Plug Flow Crystallization of Pharmaceutical Compounds. *Cryst. Growth Des.* **2010**, *10* (5), 2219–2228.
- (2) Lawton, S.; Steele, G.; Shering, P.; Zhao, L.; Laird, I.; Ni, X. Continuous Crystallization of Pharmaceuticals using a Continuous Oscillatory Baffled Crystallizer. *Org. Process Res. Dev.* **2009**, *13* (6), 1357–1363.
- (3) Vacassy, R.; Lemaitre, J.; Hofmann, H.; Gerlings, J. H. Calcium Carbonate Precipitation Using New Segmented Flow Tubular Reactor. *AIChE J.* **2000**, *46* (6), 1241–1252.
- (4) Schiewe, J.; Zierenberg, B. *Process and Apparatus for Producing Inhalable Medicaments*. U.S. Patent US20030015194 A1, Jan 23, 2003.
- (5) Lemaitre, J.; Jongen, N.; Vacassy, R.; Bowen, P. *Production of Powders*. U.S. Patent US6458335 B1, Oct 1, 2002.
- (6) Méndez del Río, J. R.; Rousseau, R. W. Batch and Tubular-Batch Crystallization of Paracetamol: Crystal Size Distribution and Polymorph Formation. *Cryst. Growth Des.* **2006**, *6* (6), 1407–1414.
- (7) Eder, R. J. P.; Radl, S.; Schmitt, E.; Innerhofer, S.; Maier, M.; Gruber-Woelfler, H.; Khinast, J. G. Continuously Seeded, Continuously Operated Tubular Crystallizer for the Production of Active Pharmaceutical Ingredients. *Cryst. Growth Des.* **2010**, *10* (5), 2247–2257.
- (8) Ferguson, S.; Morris, G.; Hao, H.; Barrett, M.; Glennon, B. In-Situ Monitoring and Characterization of Plug Flow Crystallizers. *Chem. Eng. Sci.* **2012**, *77*, 105–111.
- (9) Guillemet-Fritsch, S.; Aoun-Habbache, M.; Sarrias, J.; Rousset, A.; Jongen, N.; Donnet, M.; Bowen, P.; Lemaitre, J. High-Quality Nickel Manganese Oxalate Powders Synthesized in a New Segmented Flow Tubular Reactor. *Solid State Ionics* **2004**, *171* (1–2), 135–140.
- (10) Gerdtts, C. J.; Tereshko, V.; Yadav, M. K.; Dementieva, I.; Collart, F.; Joachimiak, A.; Stevens, R. C.; Kuhn, P.; Kossiakoff, A.; Ismagilov, R. F. Time-Controlled Microfluidic Seeding in nL-Volume Droplets to Separate Nucleation and Growth Stages of Protein Crystallization. *Angew. Chem., Int. Ed.* **2006**, *45* (48), 8156–8160.
- (11) Kashid, M. N.; Gerlach, I.; Goetz, S.; Franzke, J.; Acker, J. F.; Platte, F.; Agar, D. W.; Turek, S. Internal Circulation within the Liquid Slugs of a Liquid–Liquid Slug-Flow Capillary Microreactor. *Ind. Eng. Chem. Res.* **2005**, *44* (14), 5003–5010.
- (12) Berglund, K. A. Analysis and Measurement of Crystallization Utilizing the Population Balance. In *Handbook of Industrial Crystallization*, 2nd ed.; Myerson, A. S., Ed.; Butterworth-Heinemann: Boston, 2002; pp 104–113.
- (13) Yonemoto, T.; Kubo, M.; Doi, T.; Tadaki, T. Continuous Synthesis of Titanium Dioxide Fine Particles Using a Slug Flow Ageing Tube Reactor. *Chem. Eng. Res. Des.* **1997**, *75* (4), 413–419.
- (14) Kubo, M.; Yonemoto, T. Continuous Synthesis of TiO₂ Fine Particles and Increase of Particle Size Using a Two-Stage Slug Flow Tubular Reactor. *Chem. Eng. Res. Des.* **1999**, *77* (4), 335–341.
- (15) Dukler, A. E.; Moalem Maron, D.; Brauner, N. A. Physical Model for Predicting the Minimum Stable Slug Length. *Chem. Eng. Sci.* **1985**, *40* (8), 1379–1385.
- (16) Triplett, K. A.; Ghiaasiaan, S. M.; Abdel-Khalik, S. I.; Sadowski, D. L. Gas–Liquid Two-Phase Flow in Microchannels Part I: Two-Phase Flow Patterns. *Int. J. Multiphase Flow* **1999**, *25* (3), 377–394.
- (17) Zhao, C.; Middelberg, A. P. J. Two-Phase Microfluidic Flows. *Chem. Eng. Sci.* **2011**, *66* (7), 1394–1411.
- (18) Gopal, M.; Jepson, W. P. The Study of Dynamic Slug Flow Characteristics Using Digital Image Analysis—Part I: Flow Visualization. *J. Energy Resour. Technol.* **1998**, *120* (2), 97–101.
- (19) Günther, A.; Jhunjhunwala, M.; Thalmann, M.; Schmidt, M. A.; Jensen, K. F. Micromixing of Miscible Liquids in Segmented Gas-Liquid Flow. *Langmuir* **2005**, *21* (4), 1547–1555.
- (20) Jiang, M.; Wong, M. H.; Zhu, Z.; Zhang, J.; Zhou, L.; Wang, K.; Ford Versypt, A. N.; Si, T.; Hasenberg, L. M.; Li, Y.; Braatz, R. D. Towards Achieving a Flattop Crystal Size Distribution by Continuous Seeding and Controlled Growth. *Chem. Eng. Sci.* **2012**, *77*, 2–9.
- (21) Kuhn, S.; Hartman, R. L.; Sultana, M.; Nagy, K. D.; Marre, S.; Jensen, K. F. Teflon-Coated Silicon Microreactors: Impact on Segmented Liquid-Liquid Multiphase Flows. *Langmuir* **2011**, *27* (10), 6519–6527.
- (22) Ghajar, A. J. Non-Boiling Heat Transfer in Gas-Liquid Flow in Pipes - A Tutorial. *J. Braz. Soc. Mech. Sci.* **2005**, *27* (1), 46–73.
- (23) Fujiwara, M.; Chow, P. S.; Ma, D. L.; Braatz, R. D. Paracetamol Crystallization Using Laser Backscattering and ATR-FTIR Spectroscopy: Metastability, Agglomeration, and Control. *Cryst. Growth Des.* **2002**, *2* (5), 363–370.
- (24) Snyder, R. C.; Studener, S.; Doherty, M. F. Manipulation of Crystal Shape by Cycles of Growth and Dissolution. *AIChE J.* **2007**, *53* (6), 1510–1517.
- (25) Jiang, M.; Zhu, X.; Molaro, M.; Rasche, M.; Zhang, H.; Chadwick, K.; Raimondo, D.; Kim, K.; Zhou, L.; Wong, M.; Zhu, Z.; O'Grady, D.; Hebrault, D.; Tedesco, J.; Braatz, R. D. Modification of Crystal Shape through Deep Temperature Cycling. In revision.
- (26) Baldyga, J.; Orciuch, W. Barium Sulphate Precipitation in a Pipe — an Experimental Study and CFD Modelling. *Chem. Eng. Sci.* **2001**, *56* (7), 2435–2444.
- (27) Mahesh, K. The Interaction of Jets with Crossflow. *Annu. Rev. Fluid Mech.* **2013**, *45*, 379–407.
- (28) Eder, R. J. P.; Schmitt, E. K.; Grill, J.; Radl, S.; Gruber-Woelfler, H.; Khinast, J. G. Seed Loading Effects on the Mean Crystal Size of Acetylsalicylic Acid in a Continuous-Flow Crystallization Device. *Cryst. Res. Technol.* **2011**, *46* (3), 227–237.
- (29) Jongen, N.; Donnet, M.; Bowen, P.; Lemaitre, J.; Hofmann, H.; Schenk, R.; Hofmann, C.; Aoun - Habbache, M.; Guillemet-Fritsch, S.;

Sarrias, J.; Rousset, A.; Viviani, M.; Buscaglia, M. T.; Buscaglia, V.; Nanni, P.; Testino, A.; Herguijuela, R. Development of a Continuous Segmented Flow Tubular Reactor and the “Scale-out” Concept - In Search of Perfect Powders. *Chem. Eng. Technol.* **2003**, *26* (3), 303–305.

(30) Morari, M.; Zafiriou, E. *Robust Process Control*; Prentice Hall: Englewood Cliffs, NJ, 1989.

(31) Braatz, R. D. Internal Model Control. In *The Control Handbook*; Levine, W. S., Ed.; CRC Press: Boca Raton, FL, 1995; pp 215–224.